CORRELATION OF A NASTRAN ANALYSIS WITH TEST MEASUREMENTS FOR HEAO-2 OPTICS

Pravin K. Mehta

Electro-Optical Division, Perkin-Elmer Corporation,

Mail Station 955, 100 Wooster Heights Road, Danbury, Connecticut, 06810.

Abstract

Since achieving and maintaining the specified geometical accuracy of an optical form are important in the successful performance of an optical system, the analysis employed for the prediction of small elastic deformations of the system and/or its components must be sufficiently accurate and reliable. In this paper, the sagittal depth deviations of the paraboloids and hyperboloids of the HEAO-2 (High Energy Astronomical Observatory-2) optics are computed by NASTRAN-based finite element analysis and compared with interferometrically measured test data. The correlation between the analysis and the experiment was found to be consistently excellent. The ensuing confidence in the analysis led to analytical compensation of sagittal depth deviation in each optical element during manufacturing, practically eliminating this geometrical error from the optical form.

Introduction

The High Energy Astronomical Observatory-Mission 2 (HEAO-2), also known as the Einstein Observatory, was launched in November 1978 into earth orbit. Its mission was to perform a detailed survey and study of the galactic and extragalactic X-ray sources. R. Giacconi, the principal investigator of the mission, has described the

background and history of X-ray astronomy as well as some dramatic initial findings of the observatory in a 1980 publication.[1] The observatory consisted of the HEAO-2 spacecraft and a 58-centimeter X-ray telescope. A detailed configurational summary of the observatory has been published by R. Miller, et al.[2] The performance characteristics of the individual instruments and the scientific capabilitites of the observatory have been described by R. Giacconi, et al.[3]

The High Resolution Mirror Assembly (HRMA), one of the major subsystems of the X-ray telescope, was designed by American Science and Engineering, Inc. (AS&E). The optical elements of the HRMA were developed, manufactured, assembled, aligned and tested by the Perkin-Elmer Corporation under contract to AS&E.[4] It was an assembly of grazing incidence optics based on a Wolter-type, two-element reflecting system, in which the front element is a paraboloid and the aft element is a hyperboloid (Figure 1).[5] For increasing the net reflecting area, the HRMA included four nested, confocal, coaxial paraboloid-hyperboloid pairs of cylindrical mirrors ranging from 12.8 to 22 inches in diameter.

The reflecting elements of HRMA were fabricated from high quality fused quartz. A special Invar alloy (LR-35), which nearly matches the thermal expansion coefficient of fused quartz, was used by AS&E as the direct interface with the mirrors and the support structure. The two Invar ends were tied to the central Invar flange with thin-walled graphite-epoxy cylinders of matching expansion coefficient and superior stiffness to weight ratio. The resulting HRMA system is shown in Figure 2.

Optical Requirements and Test Plan

For high performance, each mirror was required to have a high degree of geometrical precision. Tight tolerances were specified on roundness, average radius change, forward-aft difference in average radii, circumferential variation in ΔR (i.e., $\Delta(\Delta)R$), axial slope error, azimuthal slope error, axial figure error and rms surface roughness. A good deal of our analytical and experimental work focused on containing the axial figure error (defined as the sagittal depth deviation from the ideal design curve of the optical surface) within the specified tolerance of $\pm 5 \times 10^{-6}$ inches. This accounted for the combined effect of all possible sources of figure error, such as manufacturing imperfection, metrology or figure measurement error, assembly or g-release, alignment and temperature variations.

For a number of reasons, including repeatability and minimization of self-weight induced deformation, it is a common practice to place the mirror on a specially designed support hardware after each polishing cycle, while making interferometric surface measurements. This support is commonly known as the metrology mount or "met-mount." A widely used met-mount for ultra-high precision large optics, such as the 96-inch primary mirror of the Space Telescope (manufactured by Perkin-Elmer), is a multi-point mount in which each support point provides a precalculated support force to maintain the figure of the mirror with minimum rms distortion in the earth gravitational environment. An advantage of such a deterministic met-mount is the ability to provide not only an optimum multi-point support force field taking into account the weight and stiffness variations in the mirror, but also the magnitude and location sensitivity effects of this force field. However, this type of mount is expensive and somewhat cumbersome. There are several other types of met-mounts with different advantages and disadvantages, but none particularly well-suited to our task.

The test plan for the measurement of axial figure required axial interferometric scanning of the optical surface along twelve equally spaced azimuthal stations (30^{o} apart) or meridians for each mirror. For convenience and simplicity of the test set-up, the mirror was supported on two V-blocks along its length in a horizontal orientation of the optical axis (Figure 3). Each meridian along which the optical surface was scanned was brought to the bottommost position by rotating the mirror about its axis. Since the mirror elastically deformed due to its own weight producing a sag along the scanned meridian, the interferometric data did not provide a true indication of the actual surface. If the magnitude of the gravitational sag is less than the allocated error tolerance, the presence of sag in the measurement is immaterial. Otherwise, the data reduction must compensate for this sag by subtracting it from the measurement. This technique, which may be called "Analytical Compensation", is uncommon, but is justifiable if the analysis is substantiated by consistent correlation with measured data to the required level of precision. We set out to investigate this.

Finite Element Modeling

The first step was the development of a suitable finite element model. There were eight mirrors in the HRMA system - four paraboloids and four hyperboloids of different diameters. Each mirror was a thin-walled conical shell of nominal 1/2-inch wall thickness (Figure 4). The wall thickness was actually somewhat non-uniform due to small parabolic or hyperbolic curvature of the inner reflecting surface and a zone of cylindrical outer surface at each end, which were added for the convenience of assembly. The required length of each finished mirror was 20.1 inches. An extra two inches, added in each mirror blank for the convenience of optical manufacturing, were later cut off prior to assembly. Table 1 lists the nominal values of the entrance and exit diameters defined in Figure 4.

The finite element models of the mirrors were made with the quadrilateral bending and linear strain membrane plate elements of the MSC/NASTRAN, i.e., QDPLT and QDMEM1 elements. The QUAD4 and QUAD8 elements were not available at the time. The models and the associated bulk data deck card images were generated by a specially developed, simple Fortran routine tailored to provide the flexibility needed for changing the size (degrees of freedom) of the model and various modeling parameters, such as the mirror geometries, distance between the two V-block supports, width of each support, and stiffness-equivalent thicknesses for each element to account for non-uniform wall thickness. Figure 5 shows one of the early versions of the model in which the widths of the two narrow bands of elements, distance d apart, were equal to and aligned with those of the support blocks. In this case, there was a line contact between the mirror and the V-block. For reasons, which will be explained later, the flat supporting surface of the V-block was later altered to a curved or semi-cylindrical shape, so that there was only a point contact between the mirror and the V-block at two locations, distance d apart as shown in Figure 6. In a later standardized version shown in Figure 7, the axial spacing of grid points was made more or less uniform.

The stiffness-equivalent thicknesses for each element were formulated as follows: Let

$\Delta z = z_{n+1} - z_n$ = width of the n-th axial element

$r_o = r_o(z)$ = radius from the optical axis to the outer surface

$r_i = r_i(z)$ = radius from the optical axis to the inner suface

Then

$t = t(z) \simeq r_o(z) - r_i(z)$, ignoring the small cone angle

Then

t_m = equivalent membrane thickness

$$= \frac{1}{\Delta z} \int_z t\,dz = \frac{1}{z_{n+1} - z_n} \int_{z_n}^{z_{n+1}} (r_o - r_i)\,dz \tag{1}$$

t_b = equivalent bending thickness =

$$\left[\frac{1}{\Delta z} \int_z t^3\,dz\right]^{1/3} = \left[\frac{1}{z_{n+1} - z_n} \int_{z_n}^{z_{n+1}} (r_o - r_i)^3\,dz\right]^{1/3} \tag{2}$$

t_s = equivalent tranverse shear thickness = $5t_m/6$

Due to symmetry about the vertical diametral plane, the finite element model(s) consisted of only one half of the mirror. It was also assumed that the V-blocks were rigid.

Test Set-up

The optical figure of each mirror was measured by interferometric comparison of a test plate of known (calibrated) shape with the mirror surface. The test plates, one for each mirror, consisted of prismatic bars with a "toroid" surface on one face and a flat surface on the other face, and were somewhat longer than the 24-inch length of the mirrors. With the mirror supported on two V-blocks as shown in Figure 3, the toroidal test plate was positioned above the inner surface of the mirror along the bottom meridian and a semi-automated fringe scanning was performed along the length of the mirror. This generated a punched paper tape of measured data which was fed into a computer for automatic data reduction.

The toroidal test plates were tested and certified to ensure that they would meet the desired 2×10^{-6} inch tolerance, the maximum permissible measurement error.[6]

More details of the test set-up can be found in some project reports.[4,6]

Correlation With Test

The primary objective of the interferometric test set-up was the measurement of the optical figure of each X-ray mirror. However, the measurements became "contaminated" with the gravitational sag. It was required to analytically determine and experimentally verify the gravitational sag, so that the measurements could be "purified". Therefore, for the task on hand, the requirement was quite the opposite, namely, to eliminate the polishing error from the measurement reducing it to just the gravitational sag. Fortunately, this happened to be quite simple. The polishing error remaining after a polishing cycle did not change, as the support distance d was changed, but the gravitational sag did. Therefore, the polishing error was eliminated by subtracting the gross measurement corresponding to one value of d from that for another value of d. Formalizing this, let us define, for k = 1 and 2,

$u_k = u_k(z)$ = gross measurement for $d = d_k$

$u_{g_k} = u_{g_k}(z)$ = gravitational sag for $d = d_k$

$u_p = u_p(z)$ = polishing error, independent of d.

Then

$$u_k = u_{g_k} + u_p$$

Therefore,

$$u_{g_1} - u_{g_2} = u_1 - u_2 = u_{diff} \tag{3}$$

It was this difference between two sets of measurements that was compared with the corresponding analytical difference in gravitational sag. The two values of d were: $d_1 = 13.0"$ and $d_2 = 19.1"$ or $20.1"$.

As a compromise in size between the largest and the smallest mirrors, paraboloid No. 3 was selected for the initial correlation study (Figure 1). At the outset, the V-blocks had flat plane supporting surfaces of 1-inch width producing a straight line contact with the mirror at each support location. Since the contact pressure distribution was unknown, there were several possibilities for support constraints assuming the V-blocks as rigid:

(1) radial displacement = 0 (No friction)

(2) radial displacement = 0, circumferential displacement = 0 due to friction

(3) vertical displacement = 0.

For $d = d_1$ and $d = d_2$, the gravitational sag was computed using model version 1 (Figure 5), assuming the first two sets of support constraints. In each case, the two narrow bands of elements were aligned with the V-block supports by appropriate axial shifting of some grid circles. Further, for simplicity, the inner paraboloidal surface was approximated with a conical surface generated by the rotation, about the optical axis, of a straight line passing through radii a_2 and a_3 (Figure 4). The resulting differences in the analytical gravitational sag along the test meridan were plotted in Figure 8 together with the corresponding measured data. It was clearly evident from these plots that the frictionless support contact gave a much closer correlation with the measurements than the frictional support contact. Yet the difference between the analysis and measurements was approximately $\pm 10 \times 10^{-6}$ inch, which was much too large in view of the $\pm 5 \times 10^{-6}$ inch tolerance specification on the sagittal depth deviation.

To minimize the uncertainties, such as the unknown contact pressure distribution and friction associated with the line support contact, the support surfaces of the V-block were altered from flat to curved (cylindrical) and coated with a dry lubricant. The modified V-blocks had point support contacts with the mirror and

significantly reduced friction. The assumption of frictionless support and the associated constraint only on the radial displacement was now more justifiable than before. Additionally, the approximation made previously about the inner surface of the mirror was dropped so the r_i in eqs. (1) and (2) would truly correspond to a paraboloidal surface. The analytical modifications were incorporated in the model of version 2, shown in Figure 6. These modifications in the test set-up and the finite element model led to a tremendous improvement in correlation between the two. In fact, as the plotted data for meridian No. 1 in Figure 9 shows, the agreement between the analysis and test was practically exact within the $\pm 2 \times 10^{-6}$ inch measurement uncertainty.

At this stage, it was decided to standardize the model by making the width of all the finite elements more or less uniform. The standard version (i.e., version 3) of the finite element model of paraboloid No. 3 is shown in Figure 7. Using the gravitational sagittal depth difference data computed from this model, the correlation with the measured data for meridian No. 5 was examined. The agreement between the two was again practically exact, within the known uncertainty of measurements, as shown in Figure 10.

For additional verification of the model, measurements were made on one of the largest mirrors in the HRMA subsystem, namely, hyperboloid No. 1. It may be recalled that all the hyperboloids were axially more tapered than the paraboloids (see Table 1). The analytical data and measurements for meridian 1 and 7 were compared. As shown in Figures 11 and 12, the correlation between the measurements and analysis was once again excellent.

Concluding Remarks

The correlation of analytical predictions of the finite element models with the measurements, and the resulting confidence in the models, led to several benefits.

- No multi-point or other complicated metrology mount was required during the axial figure metrology operations, because analytical compensation was quite reliable for HEAO-2 X-ray mirrors, permitting the analytical gravitational sag to be subtracted from the measurements during the computerized reduction of interferometric data.
- Since the analytical predictions for gravitational sag during the axial figure metrology operations were accurate within the measurement uncertainty of $\pm 2 \times 10^{-6}$ inch, most of the remainder of the allocated error budget of $\pm 5 \times 10^{-6}$ inch was available to the design of the zero-g fixture required for the assembly and alignment phase of the HRMA subsystem.
- With the largest share of error allocation at its disposal, the multi-point zero-g fixture required fewer points to support each mirror during assembly than would otherwise be required. This reduced the complexity of the fixture and its sensitivity to off-nominal deviations of the computed multipoint support forces.
- In view of the confidence established in the finite element model for predicting gravitational sag, there was good reason to be confident in FEM analysis for interspan gravitational sag of each mirror supported during assembly on a 32-point zero-g fixture, the associated computations for the support forces and the sensitivity analysis.[4]

As mentioned earlier, the finite element models of the X-ray telescope mirrors employed QDPLT and QDMEM1 quadrilateral plate elements of MSC/NASTRAN, because QUAD4 and QUAD8 were not then available in the element library of the

program. When the QUAD4 element became available, a test run was made for paraboloid No. 3 with a model made of QUAD4 elements. Practically no change was observed in the results.

Acknowledgments

HEAO was a NASA program managed by Marshall Space Flight Center. Scientific requirements were established by a consortium comprised of the Smithsonian Astrophysical Observatory, MIT, Columbia University and the Goddard Space Flight Center. The prime contractor for the HEAO spacecraft was TRW Inc., and that for the X-ray telescope was American Science and Engineering, Inc., (AS&E). The work presented in this paper was performed under AS&E contract no. 80228-8 (1975-76).

TABLE 1: NOMINAL VALUES OF THE MIRROR ENTRANCE AND EXIT DIAMETERS*

REFLECTING SURFACE		$2a_1$ inch	$2a_2$ inch	$2a_3$ inch	$2a_4$ inch
TYPE	NO.				
Paraboloid	1	23.7583	22.8378	22.0366	23.1165
	2	20.4268	19.4948	18.8107	19.8789
	3	17.2417	16.2985	15.7266	16.7836
	4	14.1957	13.2419	12.7772	13.8235
Hyperboloid	1	22.6456	21.8901	19.4170	20.6652
	2	19.4685	18.6773	16.5669	17.7784
	3	16.4346	15.6093	13.8454	15.0219
	4	13.5363	12.6783	11.2455	12.3887

*See Figure 4

TABLE 1: NOMINAL VALUES OF THE MIRROR ENTRANCE AND EXIT DIAMETERS*

REFLECTING SURFACE		$2a_1$ inch	$2a_2$ inch	$2a_3$ inch	$2a_4$ inch
TYPE	NO.				
Paraboloid	1	23.7583	22.8378	22.0366	23.1165
	2	20.4268	19.4948	18.8107	19.8789
	3	17.2417	16.2985	15.7266	16.7836
	4	14.1957	13.2419	12.7772	13.8235
Hyperboloid	1	22.6456	21.8901	19.4170	20.6652
	2	19.4685	18.6773	16.5669	17.7784
	3	16.4346	15.6093	13.8454	15.0219
	4	13.5363	12.6783	11.2455	12.3887

*See Figure 4

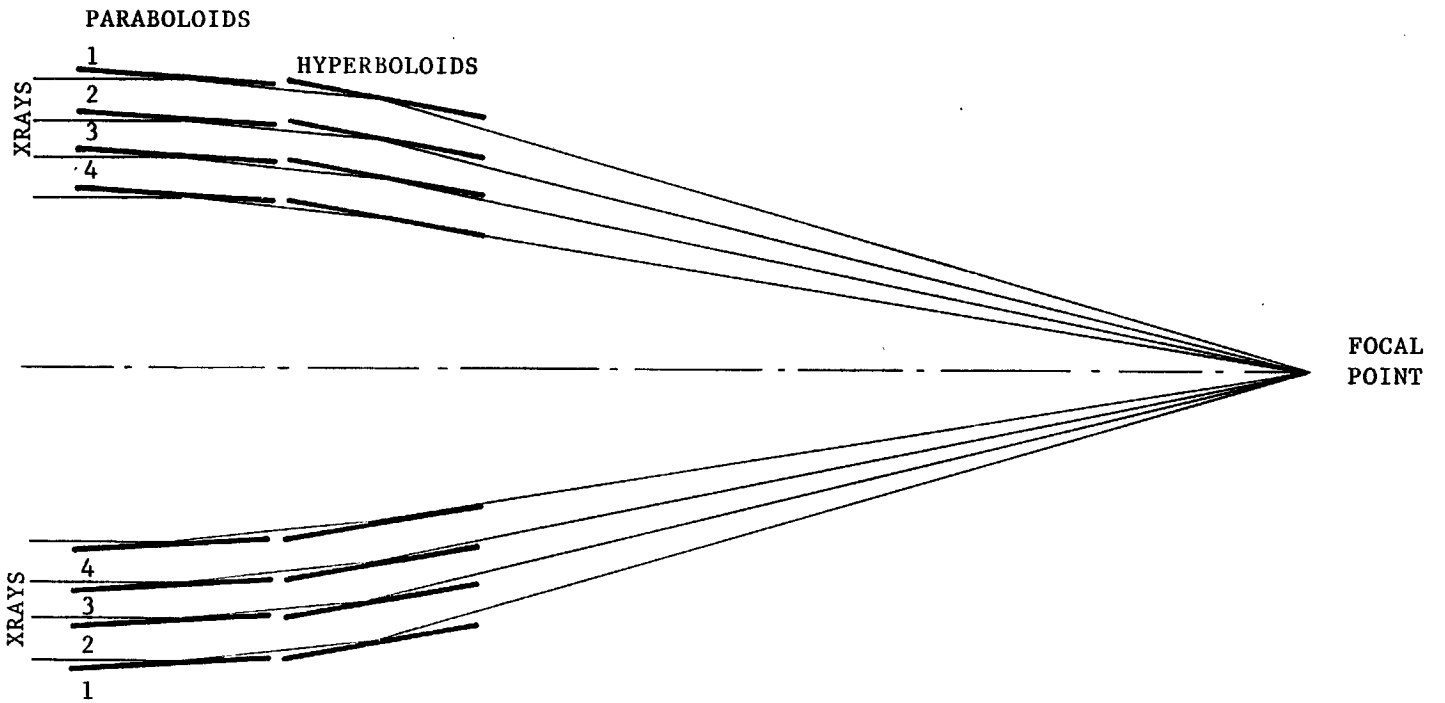

FIGURE 1: A SCHEMATIC CROSS SECTION OF THE HEAO-2 OPTICAL SYSTEM

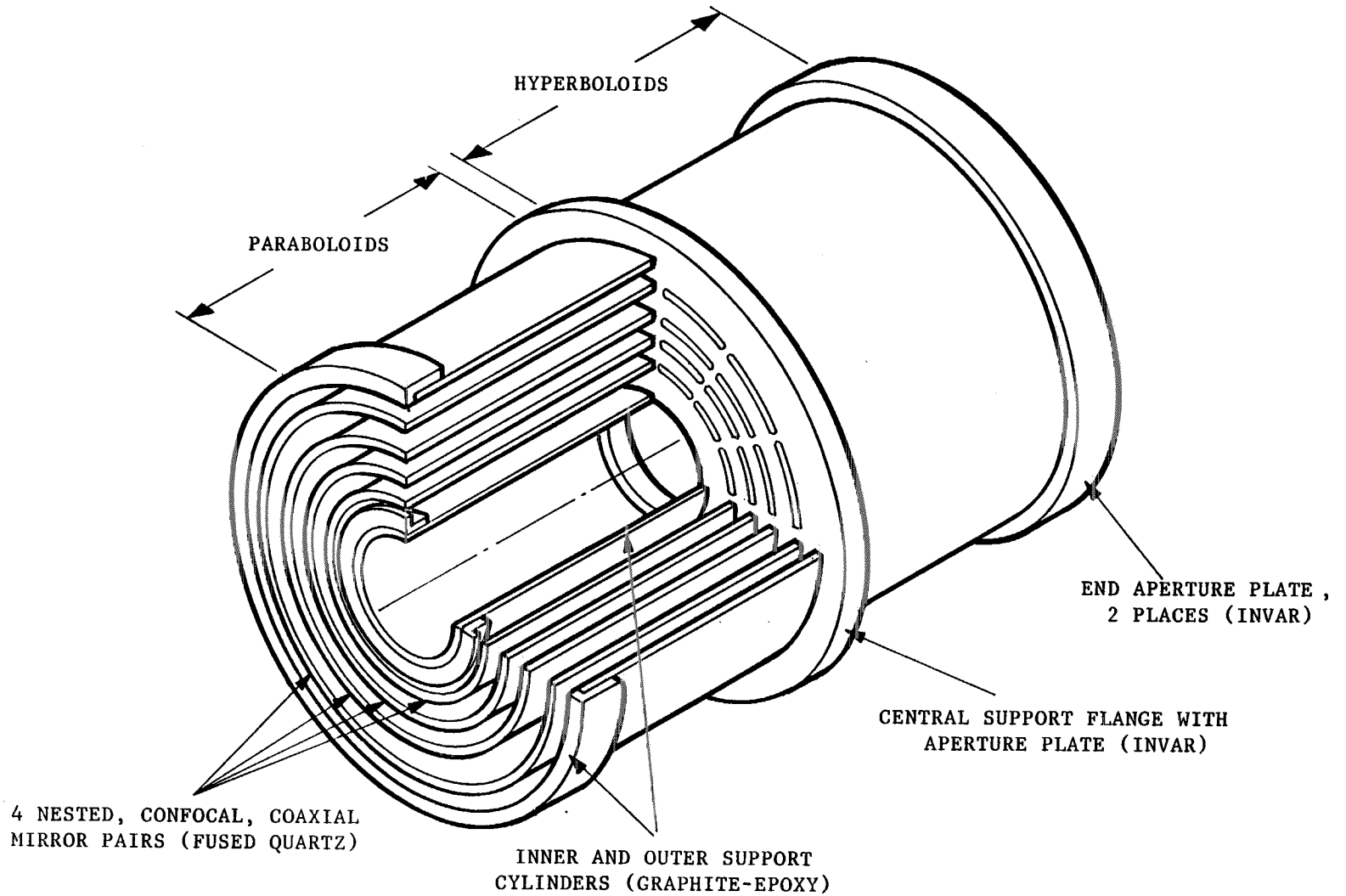

FIGURE 2: THE HIGH RESOLUTION MIRROR ASSEMBLY (HRMA)

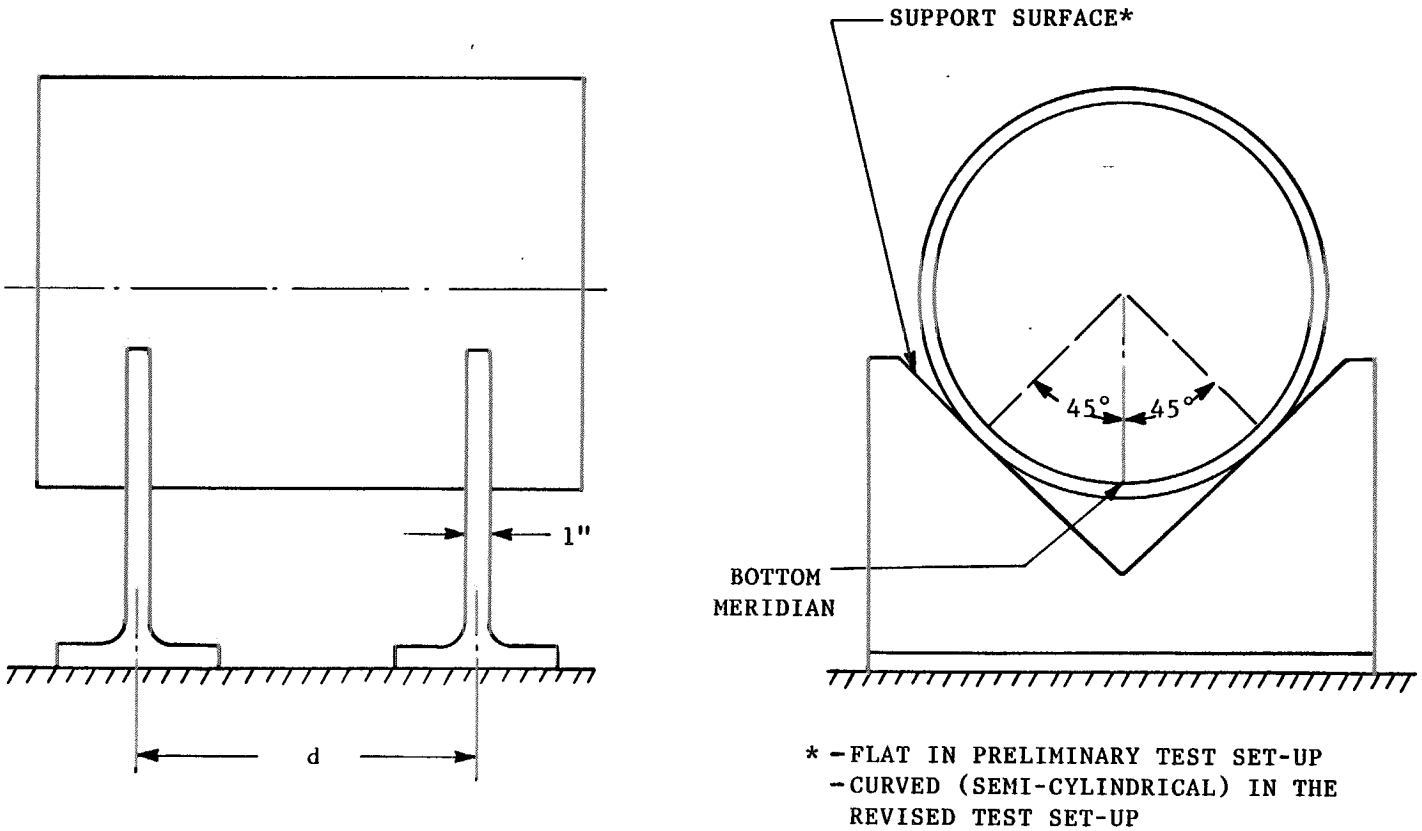

FIGURE 3: MIRROR ON V-BLOCK SUPPORTS FOR AXIAL FIGURE METROLOGY SET-UP

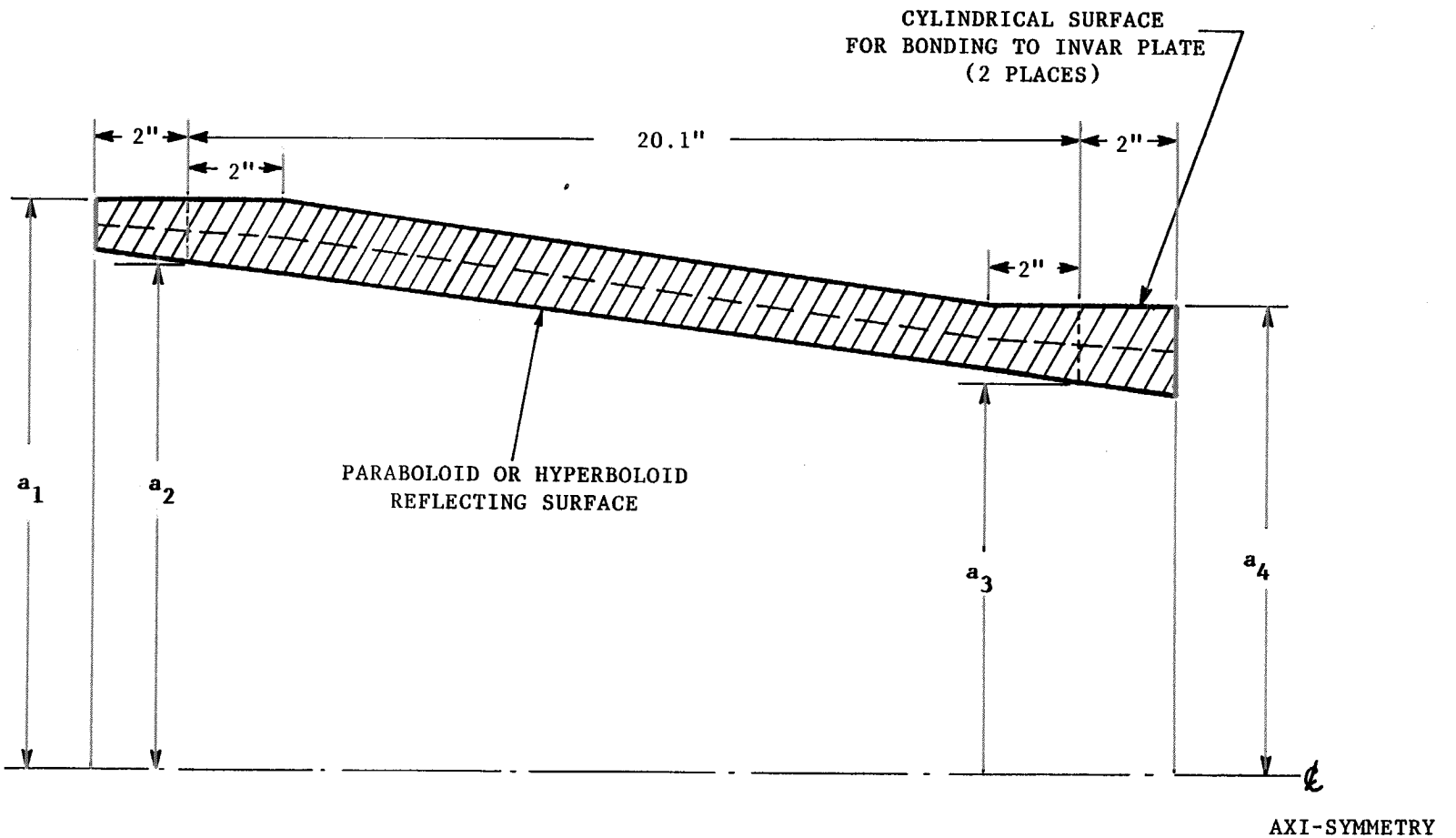

FIGURE 4: CROSS SECTION OF A TYPICAL MIRROR

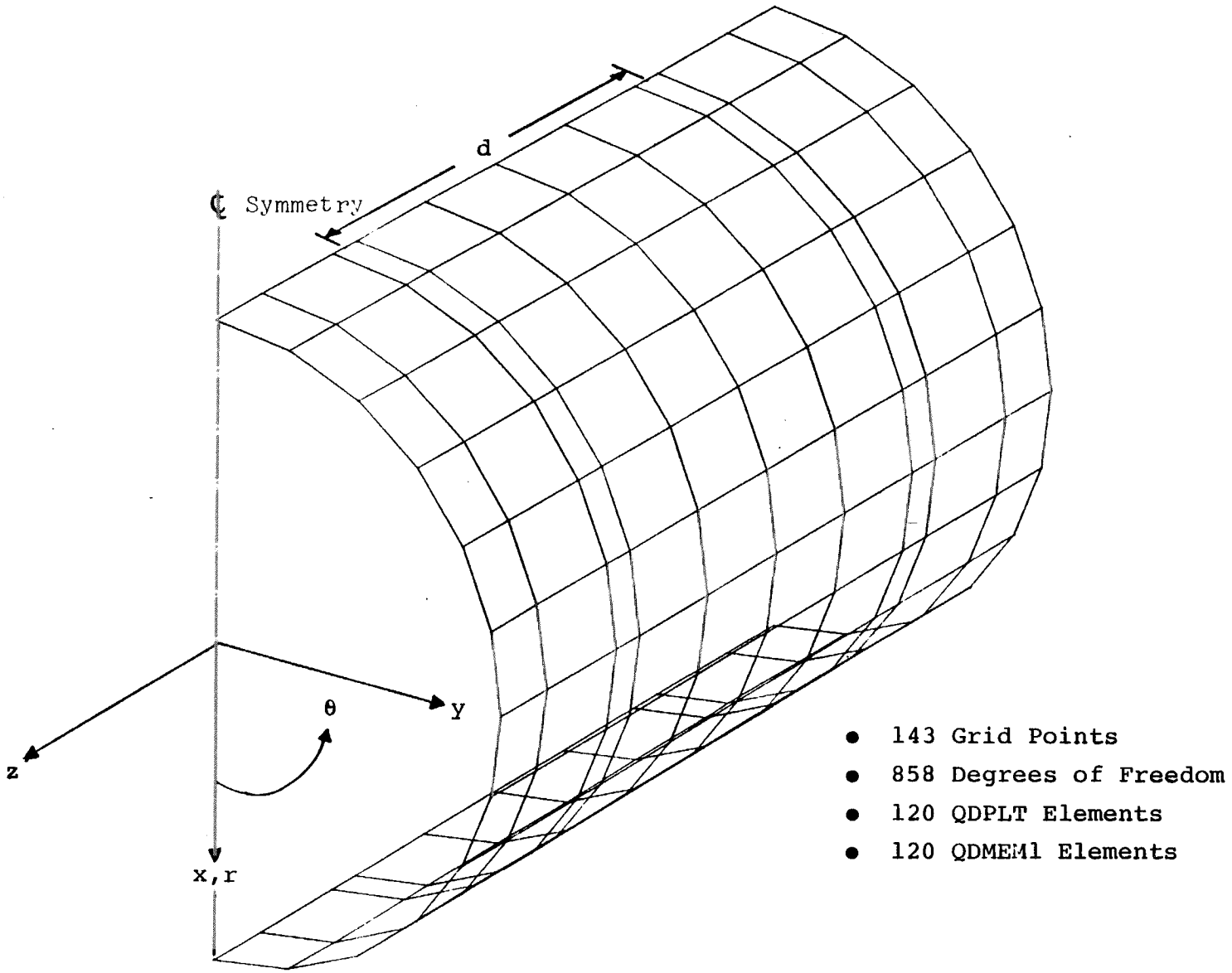

FIGURE 5: A PRELIMINARY FINITE ELEMENT MODEL OF A TYPICAL MIRROR, VERSION 1

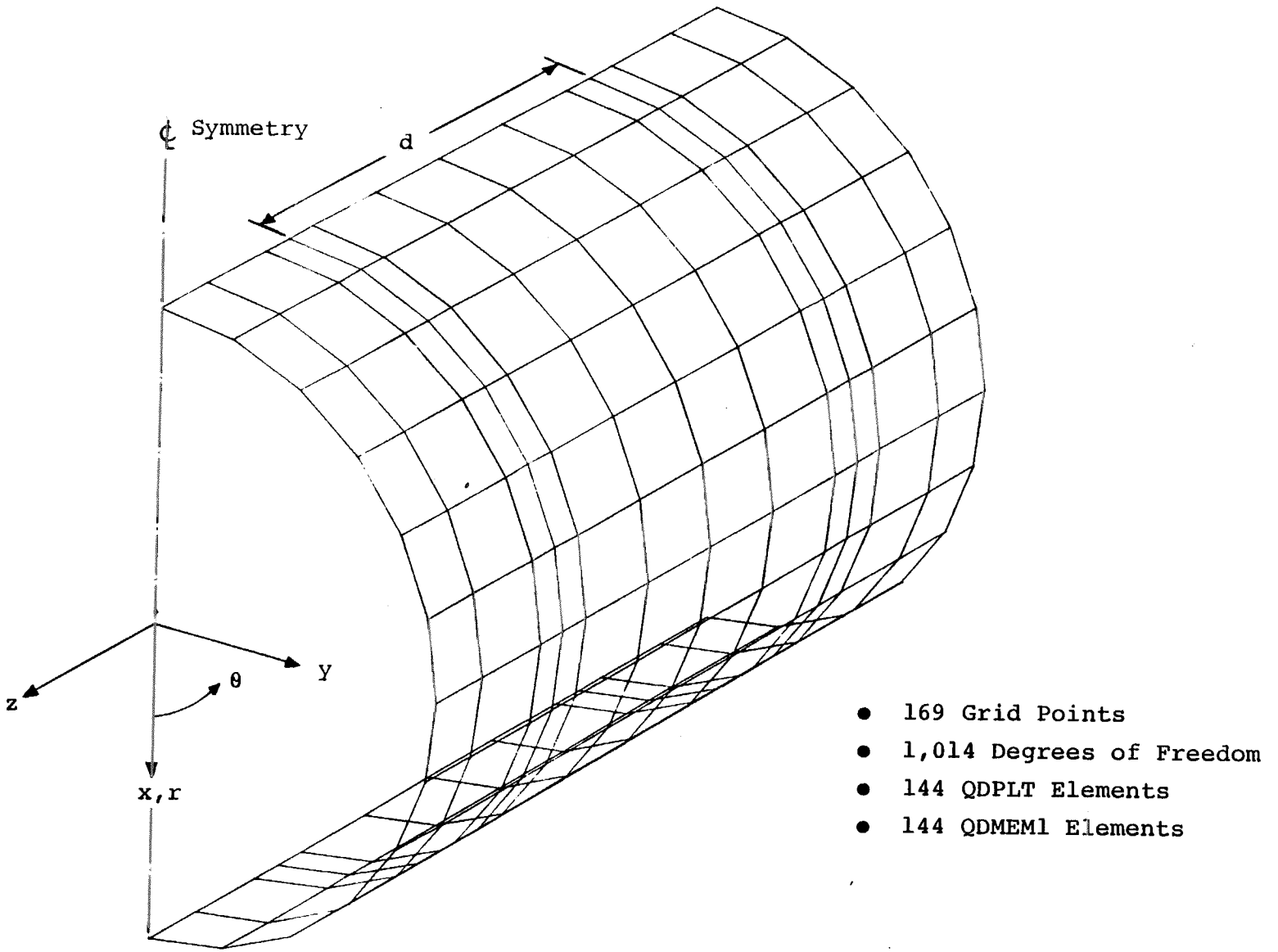

FIGURE 6: REVISED FINITE ELEMENT MODEL OF A TYPICAL MIRROR, VERSION 2

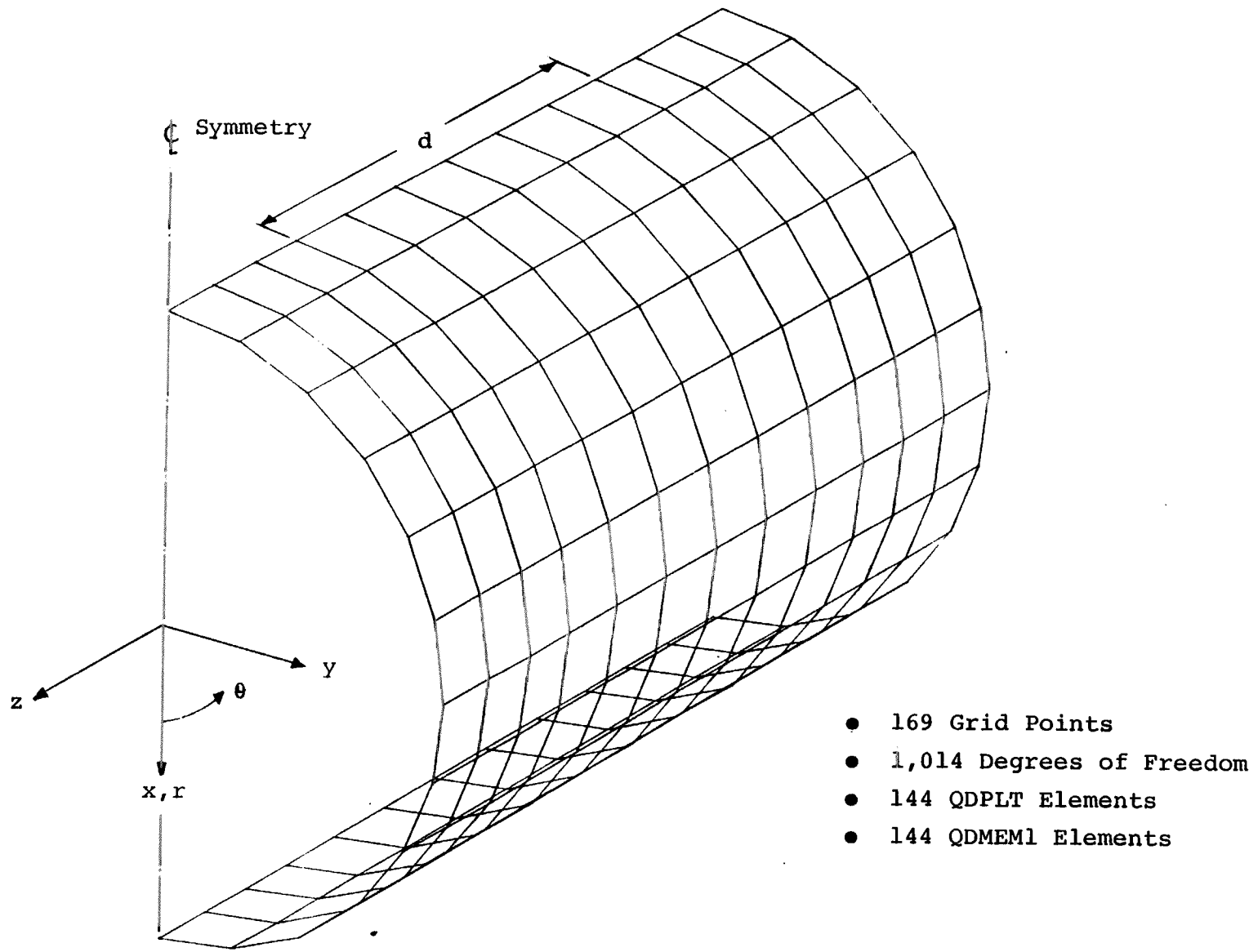

FIGURE 7: STANDARDIZED FINITE ELEMENT MODEL OF A TYPICAL MIRROR, VERSION 3

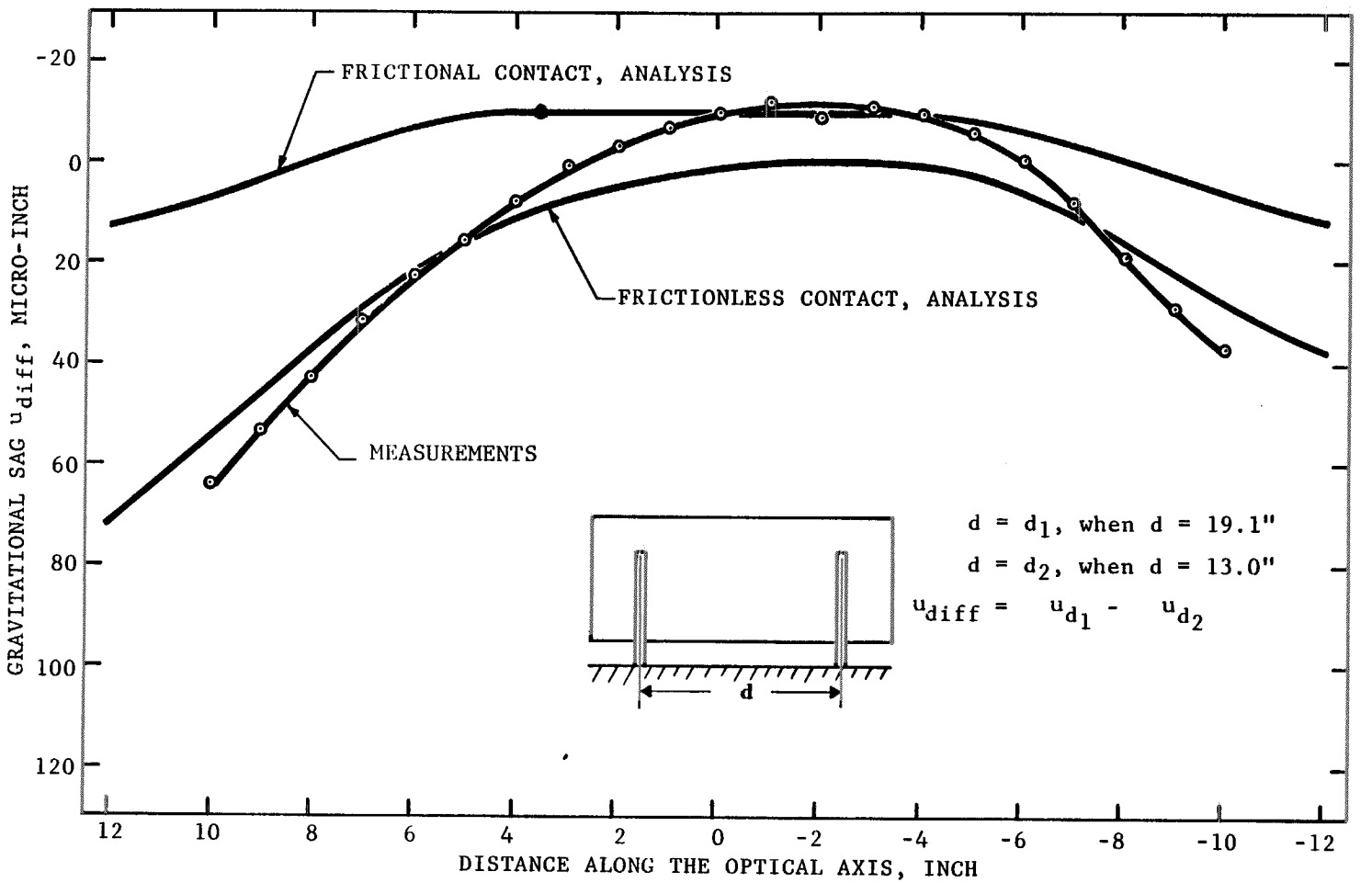

FIGURE 8: CORRELATION BETWEEN ANALYSIS AND MEASUREMENTS FOR PARABOLOID NO. 3, MERIDIAN NO. 1, BASED ON THE PRELIMINARY TEST SET-UP (V-BLOCKS WITH NON-LUBRICATED FLAT SUPPORTING SURFACES)

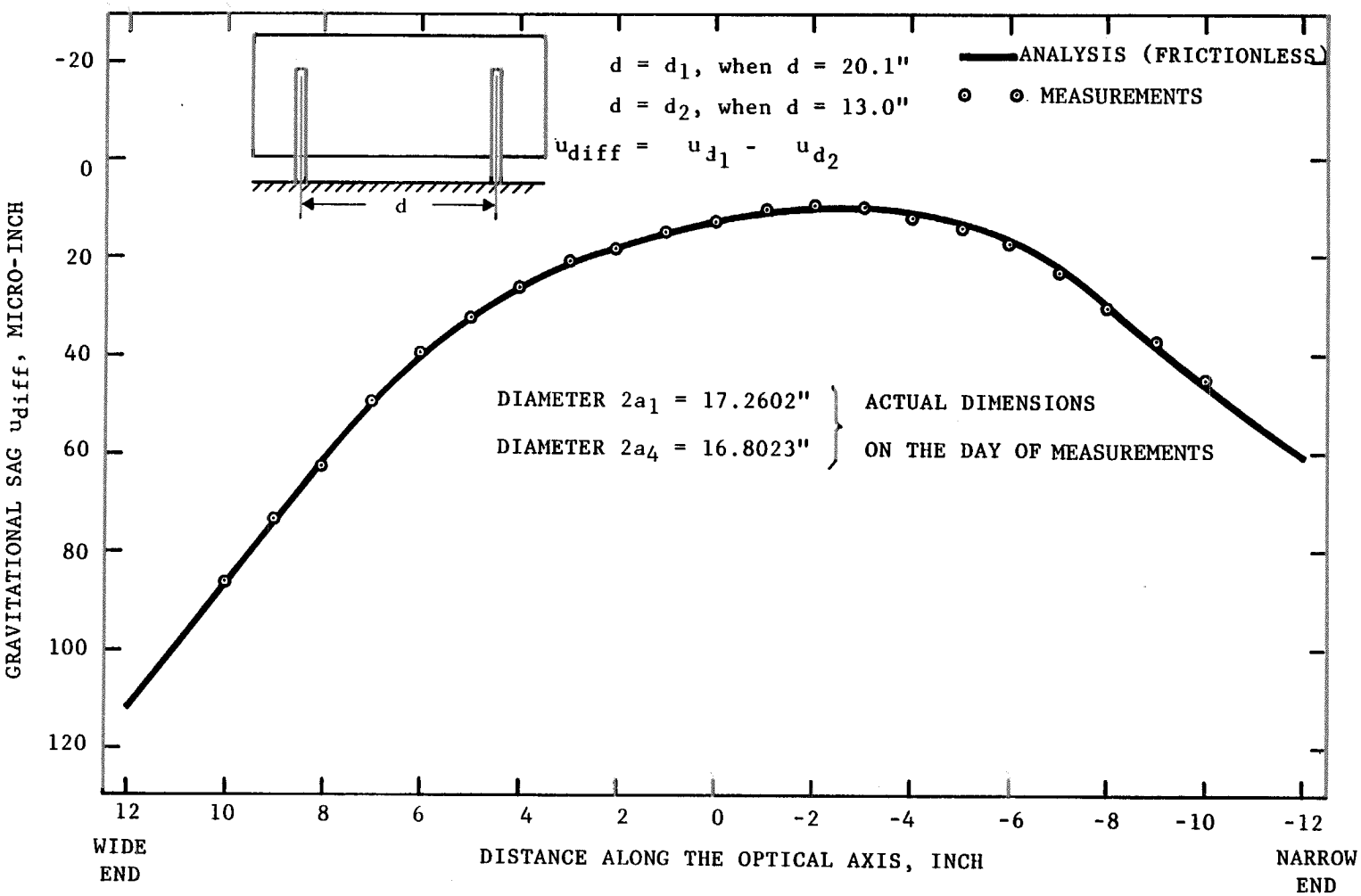

FIGURE 9: CORRELATION BETWEEN ANALYSIS AND MEASUREMENTS FOR PARABOLOID NO. 3, MERIDIAN NO. 1, BASED ON THE REVISED TEST SET-UP (V-BLOCKS WITH LUBRICATED CURVED SUPPORTING SURFACES)

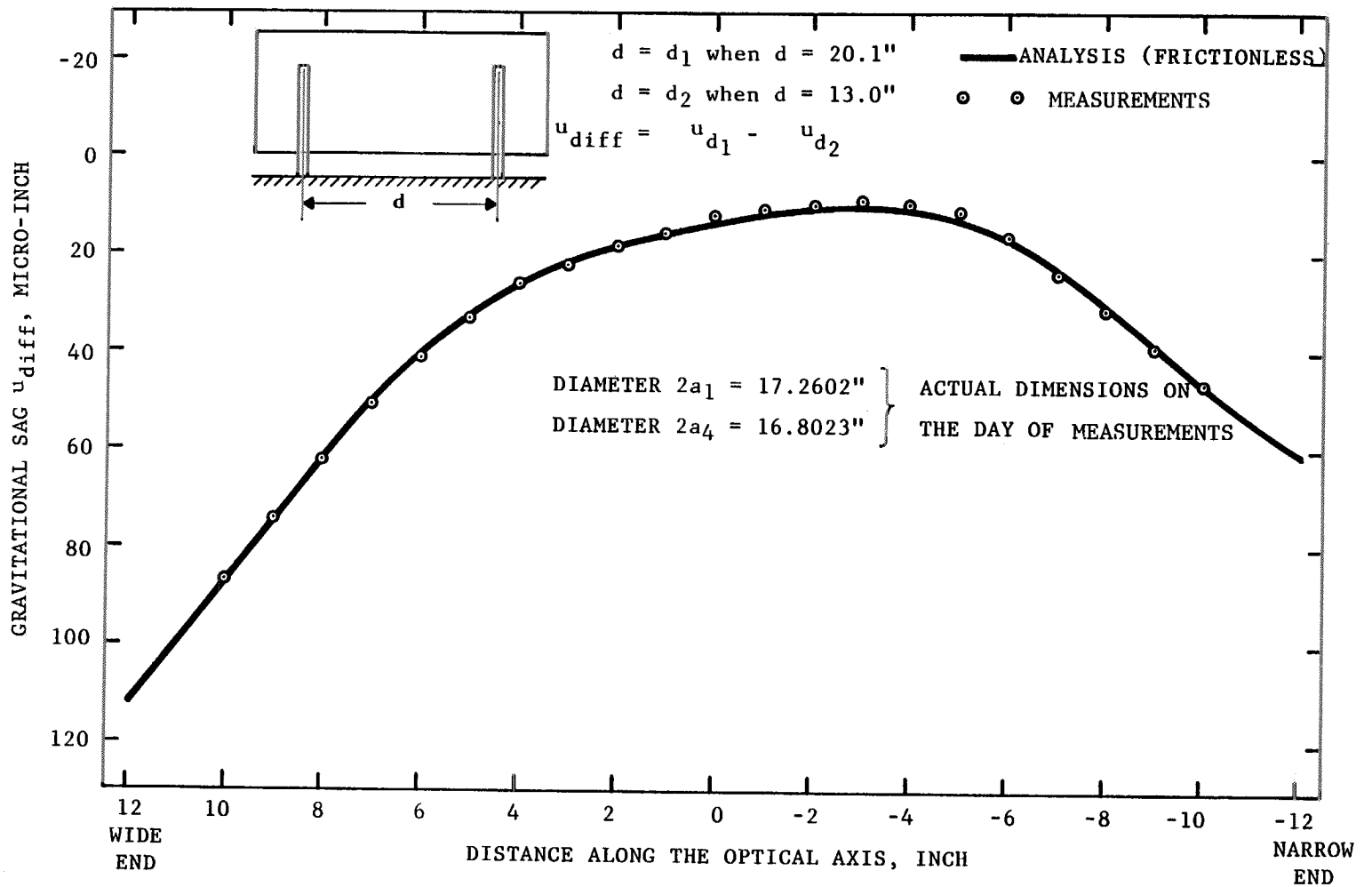

FIGURE 10. CORRELATION BETWEEN ANALYSIS AND MEASUREMENTS FOR PARABOLOID NO. 3, MERIDIAN NO. 5, BASED ON THE REVISED TEST SET-UP (V-BLOCKS WITH LUBRICATED CURVED SUPPORT SURFACES)

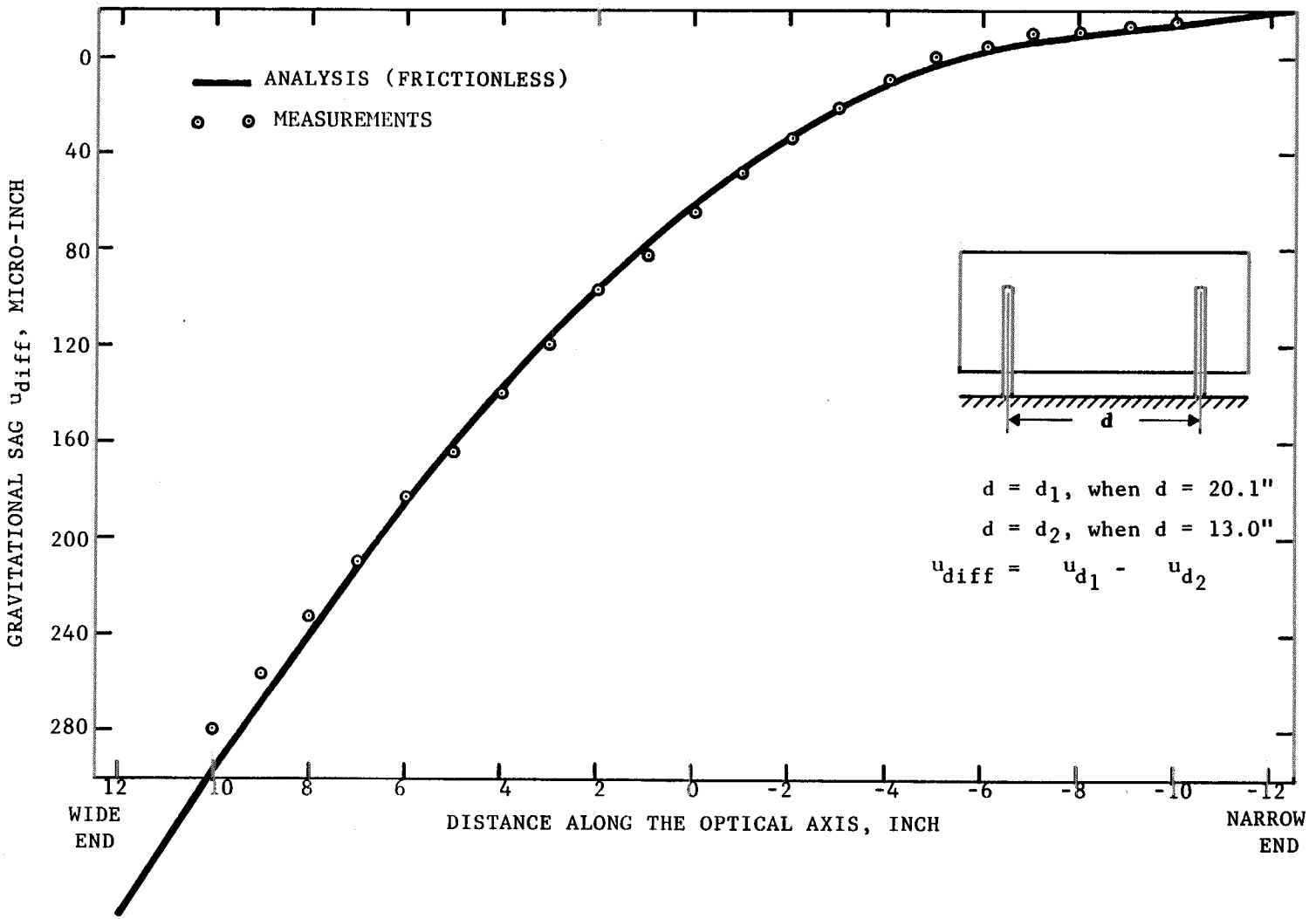

FIGURE 11. CORRELATION BETWEEN ANALYSIS AND MEASUREMENTS FOR HYPERBOLOID NO. 1, MERIDIAN NO. 1, BASED ON THE REVISED TEST SET-UP (V-BLOCKS WITH LUBRICATED CURVED SUPPORTING SURFACES)

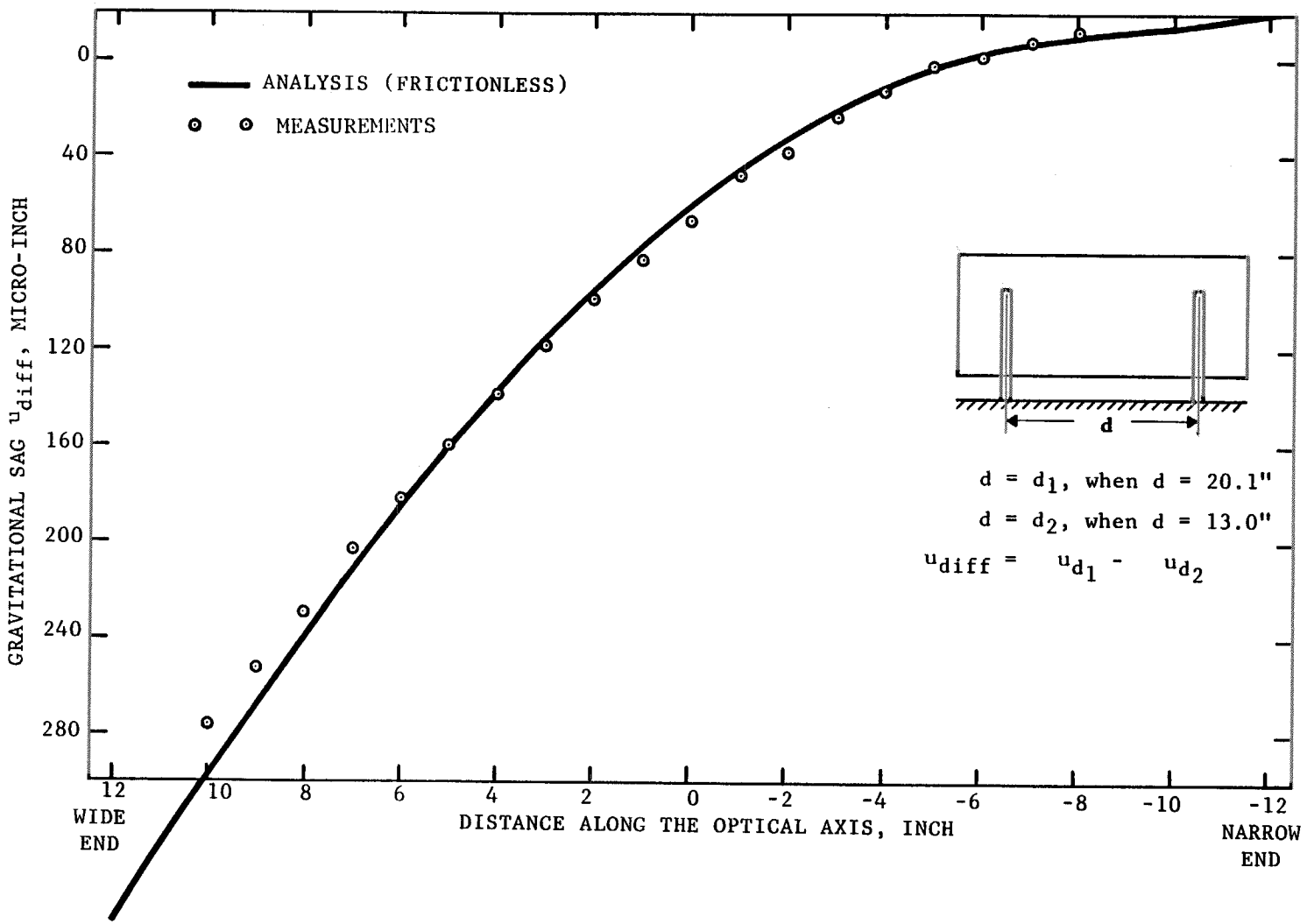

FIGURE 12: CORRELATION BETWEEN ANALYSIS AND MEASUREMENTS FOR HYPERBOLOID NO. 1, MERIDIAN NO. 7, BASED ON THE REVISED TEST SET-UP (V-BLOCKS WITH LUBRICATED CURVED SUPPORTING SURFACES)

References

1. R. Giacconi, "The Einstein X-Ray Observatory", Scientific American, Vol. 242 No. 2, pp. 80-102, February 1980.

2. R. Miller, et al, "The High Energy Astronomy Observatory X-Ray Telescope", IEE Transactions on Nuclear Sciences, Vol. NS-25, No. 1, pp. 422-429, February 1978.

3. R. Giacconi, et al, The Einstein (HEAO-2) X-Ray Observatory", The Astrophysical Journal, 230: 540-550, June 1, 1979.

4. P. Young, "HEAO-B X-Ray Telescope, Final Technical Report", The Perkin-Elmer Corporation, Report No. 13292, 17 January 1977.

5. H. Wolter, "Annalen der Physik". 10, 94, 1952.

6. J.A. Magner, "Optical Test Plate Certification Procedure", The Perkin-Elmer Corporation, Report No. 12217, May 1976.